IN-SITU MEASUREMENT OF DIFFUSE ATTENUATION COEFFICIENT AND ITS RELATIONSHIP WITH WATER CONSTITUENT AND DEPTH ESTIMATION OF SHALLOW WATERS BY REMOTE SENSING TECHNIQUE

Budhi Agung Prasetyo[1*)], Vincentius Paulus Siregar[*)], Syamsul Bahri Agus[*)], Wikanti Asriningrum[**)]

[*)] Departmen of Marine Science and Technology, Institut Pertanian Bogor, Bogor

[**)] Remote Sensing Applications Center,

National Institute of Aeronautics and Space of Indonesia

Jl. Kalisari No.8 Kelurahan Pekayon Kecamatan Pasar Rebo Jakarta Timur, Indonesia

[1]e-mail: budhiagungp@gmail.com

Received: 9 June 2017; Revised: 15 June 2017; Approved: 18 June 2017

Abstract. Diffuse attenuation coefficient, $K_d(\lambda)$, has an empirical relationship with water depth, thus potentially to be used to estimate the depth of the water based on the light penetration in the water column. The aim of this research is to assess the relationship of diffuse attenuation coefficient with the water constituent and its relationship to estimate the depth of shallow waters of Air Island, Panggang Island and Karang Lebar lagoons and to compare the result of depth estimation from K_d model and derived from Landsat 8 imagery. The measurement of $K_d(\lambda)$ was carried out using hyperspectral spectroradiometer TriOS-RAMSES with range 320 – 950 nm. The relationship between measurement $K_d(\lambda)$ on study site with the water constituent was the occurrence of absorption by chlorophyll-a concentration at the blue and green spectral wavelength. Depth estimation using band ratio from $K_d(\lambda)$ occurred at 442,96 nm and 654,59 nm, which had better relationship with the depth from in-situ measurement compared to the estimation based on Landsat 8 band ratio. Depth estimated based on Kd(λ) ratio and in-situ measurement are not significantly different statistically. Depth estimated based on $K_d(\lambda)$ ratio and in-situ measurement are not significantly different statistically. However, depth estimation based on $K_d(\lambda)$ ratio was inconsistent due to the bottom albedo reflection because the $K_d(\lambda)$ measurement was carried out in shallow waters. Estimation of water depth based on $K_d(\lambda)$ ratio had better results compared to the Landsat 8 band ratio.

Keywords: *in-situ measurement, diffuse attenuation coefficient, relationship with water constituent, depth estimation, shallow water, remote sensing*

1 INTRODUCTION

Utilization of optically based remote sensing technology for depth mapping had a limiting factor, which is attenuation on the water column. Light intensity that penetrated on water column will exponentially decrease by the depth and another process that occurred in water columns such as absorption and scattering. It caused light transmission that carrying information back to the sensors of satellite become decreased because the interaction with water constituent (Groetsch 2011).

Information about $K_d(\lambda)$ values can be used as a basic information to assess the circumstances of water column optically. The information can also be used as the range of light penetration that can be sensed by satellite sensor, thus the accuracy of the sensed information can be improved (Kirk 2011). The previous studies about depth estimation on shallow waters using

optically based remote sensing technology stated that the water column has a unique optical properties which is attenuation (Lyzenga 1978 1981; Green *et al.* 2000; Stumpf *et al.* 2003). The previous research about depth estimation from satellite imagery also used band ratio. This method was used to normalized the existing reflection on the bottom of the sea that caused by light penetration on water column (Lyzenga 1978,1981).

One of the most commonly used band ratio methods was introduced by Stumpf *et al.* (2003), where natural logarithmic functions of each band towards the measured depth to assess the interaction of light that penetrated on water column in accordance with the Beer-Lambert law, which is attenuation. This method, however, were not applicable if the water column has a dynamics optical property. The aforementioned method required two bands from satellite imagery to calculate the attenuation.

The in-situ measurement of attenuation coefficient can be done with calculating the downwelling irradiance (E_d) on each depth inside the water column. Previous research about bottom habitat and depth estimation around Karang Lebar and Panggang Island lagoon, Siregar and Selamat (2010) stated that information about the optical properties on each area, such as attenuation coefficient, was required to improve the accuracy.

Calculating the diffuse attenuation coefficient (K_d) using in-situ measurement, need a specific device called spectro-radiometer. The availability of such device in Indonesia was still limited and rarely used. The aim of this research is to assess the relationship of diffuse attenuation coefficient with the water constituent and its relationship to estimate depth at the shallow waters of Panggang and Karang Lebar lagoons. This research were also aimed on comparing the depth estimation derived from Landsat-8 imagery and K_d.

2 MATERIALS AND METHODOLOGY

2.1 Field survey location

The field measurement was conducted on shallow waters that have various bottom types consist of seagrass and coral reefs habitat. The water depth ranged between 1 to >20 meters around Air island, Panggang island and Karang Lebar lagoonal area (Figure 2-1). The Area of study located in the longitude 5º43'00" – 5º46'00" and latitude 106º33'30" – 106º37'30". Points of field measurement determined using line transect methods. Field measurement of optical properties was conducted on 24-28 April 2016. There was six line transects which determined using stratified random sampling methods with the assumption of shallow waters around the lagoonal area has several groups of depth level, in the middle, edges and in the outside of lagoon.

2.2 Waters Characteristic Measurement

Water characteristic measurements were consist of water depth, water transparency, chlorophyll-a (Chl-a) and total suspended solid (TSS). The measurement of Chl-a and TSS were conducted to assess the influences to $K_d(\lambda)$ values that represent the absorption and scattering. Water sample was taken from one water column (bulk measurement), with Van-Dorn water sampler, so it represented each level of depth. Water transparency measured using Secchi-disc and the depth of water column measured using sounder gun. The recording of the location coordinate was carried out using handheld GPS Garmin Montana 680 with the margin of error for the exact location within 3.65 m, concurrently with the recording of the atmospheric condition and benthic types on that location. The analysis of Chl-a

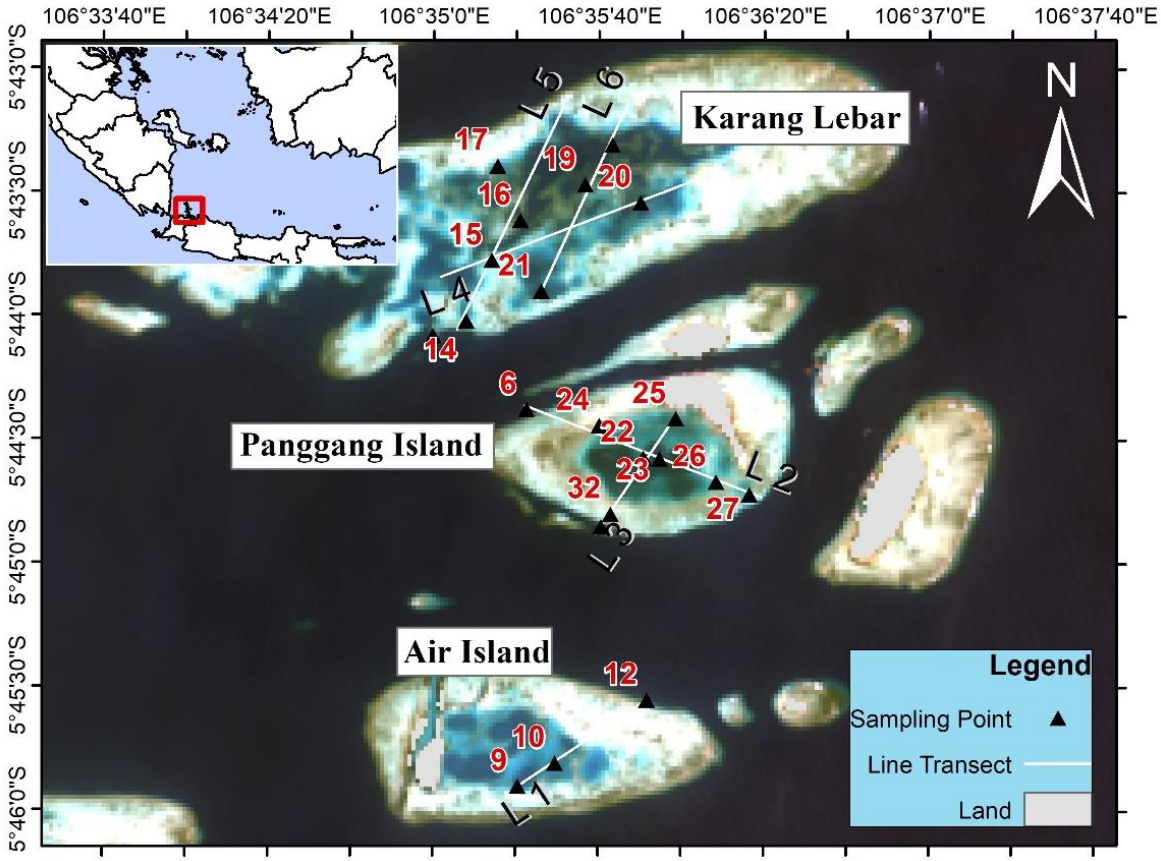

Figure 2-1: Map of field measurement (Source: Landsat 8 imagery)

was conducted on laboratory using spectrophotometry method to calculate its content. The TSS analysis was conducted by a gravimetric method for calculating the difference of weight the membrane filter. Both methods were performed in accordance with APHA (2012).

2.3 Radiometric measurement

Radiometric data were measured using three sensors from TriOS-RAMSES spectroradiometer. One of three sensors was an irradiance sensor (ACC-2-VIS), and the other two were radiance sensors (ARC-VIS) with 7° field-of-view. All sensors from TriOS-RAMSES worked in a range of 320 nm to 950 nm and spectral sampling of 3.3 nm. Data inputs to calculate diffuse attenuation coefficient was recorded from downwelling irradiances, $E_d(\lambda)$, and the irradiances sensor (ACC-2-VIS). The measurement of $E_d(\lambda)$ in the water column was performed underwater on depth Z_1 and Z_s. The sensor was pointed in 90° upward direction to collect the incident radiation (Figure 2-2b). The above-water measurement was also performed to calculate Remote Sensing Reflectance, $R_{rs}(\lambda)$. The cosine collector was pointed upward for collecting the incident sky radiation as well as underwater configuration, $E_d(\lambda)$. Meanwhile, a radiance sensor was pointed 135° in the upward direction to measure the incident sky radiance $L_{sky}(\lambda)$. The second radiance sensor was pointed 45° downward to measure the total radiance, $L_u(\lambda)$. These configuration of three sensors were in accordance by Mueller *et al.* (2003) (Figure 2-2a).

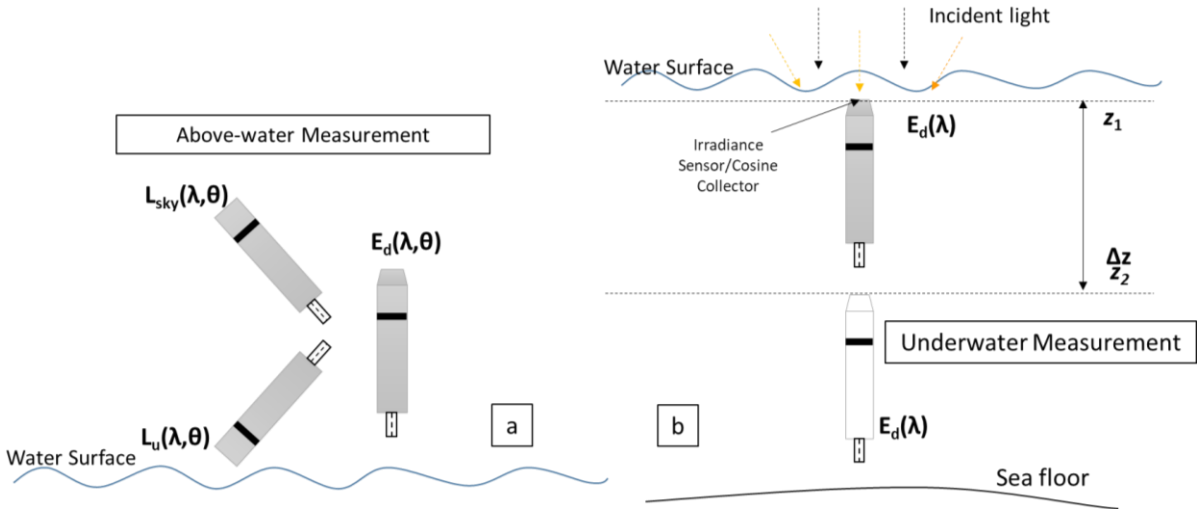

Figure 2-2: Illustration of TriOS-RAMSES's sensors configuration during field measurement; (a) measurement of $R_{rs}(\lambda)$; (b) measurement of $E_d(\lambda)$ (Prasetyo *et al.* 2017)

According to Prasetyo *et al.* (2017) the radiometric data from TriOS-RAMSES was acquired using a portable computer. The data acquired was presented as table and chart using a software called Multi-Sensor Data Acquisition (MSDA_XE ver. 8.9.2 2014-04-28) that was provided by TriOS GmbH. The data then radiometrically calibrated using its calibration files. The sensors itself calibrated with the white reference and dark reference panel provided by Remote Sensing Applications Center of National Institute of Aeronautics and Space (LAPAN) before taking the field measurement. The $E_d(\lambda)$ data then extracted from MSDA into tab-delimited format for the next process. The $E_d(\lambda)$ was plotted for curve fitting with the exponential function from the $E_d(\lambda)$ itself. Values of $K_d(\lambda)$ then can be calculated using the $E_d(\lambda)$ data on two different depth levels from RAMSES spectro-radiometer by downward irradiance on hyperspectral wavelength centered on λ (Kirk, 2011) (equation 2-1).

$$K_d(\lambda) = \frac{1}{z_2 - z_1} ln \frac{E_d(z_{1,\lambda})}{E_d(z_2,\lambda)} \qquad (2\text{-}1)$$

where, z_2-z_1 is the differences of depth level on each measurement (m), and E_d is the values of downwelling irradiance at depth z at wavelength λ.

Remote Sensing Reflectance $R_{rs}(\lambda)$ was calculated from above water measurement. It was the ratio between the water-leaving radiance ($L_w(\lambda)$) and downwelling irradiance ($E_d(\lambda)$) (Mobley 1999; Budhiman *et al.* 2012):

$$R_{rs}(\lambda) = \frac{L_w(\lambda)}{E_d(\lambda)} \qquad (2\text{-}2)$$

Water-leaving radiance, $L_w(\lambda)$, was calculated from the measurement of upwelling radiance, $L_u(\lambda)$, on the surface, where the total radiance came from water surface then sensed by the sensor, which is consisted by water-leaving radiances and sky radiance that reflected by above water surface. The water-leaving radiance itself calculated using the equation 2-3 (Mueller *et al.* 2003).

$$L_w(\lambda) = L_u(\lambda) - \rho_{sky}.L_{sky}(\lambda) \qquad (2\text{-}3)$$

with, $L_u(\lambda)$ is the upwelling radiance measurement, that is all radiance that comes from above water surface or by surface reflectance, $L_{sky}(\lambda)$ is downwelling radiance measurement that comes from the sky, $\rho_{sky}(\lambda)$ is the coefficient from water-sky interaction that can be

calculated using *Fresnel* equation (Hect 2002; Budhiman *et al.* 2012).

2.4 Landsat 8 Radiometric and Atmospheric Correction

The Landsat 8 imagery data on path/row 122/64 was acquired on Mei, 13, 2016. The acquisition date was the closest to the field measurement (15 days differences). The scene was corrected radiometrically and atmospherically to change the digital number (DN) into corrected reflectance values. The correction method was performed in accordance to Landsat 8 handbook provided by USGS (2015).

The atmospheric correction was done by performing Dark Pixel methods or Dark Object Subtraction. This atmospheric correction method used the assumption that the values of $R_{rs}(\lambda)$ which sensed by the satellite sensor was affected by atmospheric condition (Green *et al.* 2000; Vaderstraete *et al.* 2004; Budhiman *et al.* 2013). Dark Object Subtraction method used the assumption that minimum pixel values that appeared other than zero are assumed from the atmosphere. All pixels on the scene then had to be subtracted by all minimum values (Jaelani *et al.* 2015).

2.5 Depth Estimation Using Band Ratio of Landsat 8

Band ratio were used to normalize the effect of the bottom reflection that affected by light penetration through the water column. It was consist of two bands, and calculated based on Stumpf *et al.* (2003) using equation 2-4.

$$z = m_1 \frac{(\ln(nRw(\lambda_i)))}{(\ln(nRw(\lambda_j)))} - m_0 \qquad (2\text{-}4)$$

with Z is the actual depth from in-situ measurement, m_1 and m_0 is the offset and gain from a simple regression of two bands towards actual depth, ln(nRw(λ)) is the ratio band on band *i* and band *j*.

3 RESULTS AND DISCUSSION

3.1 Diffuse Attenuation Coefficient $K_d(\lambda)$

The measurement of $K_d(\lambda)$ was conducted to assess the variability of optical properties in three lagoonal areas. According to Prasetyo *et al.* (2017) the results of measurement on each point in the middle part of Karang Lebar lagoon, generally has the same pattern with Air Island and Panggang island lagoon. The averages of $K_d(\lambda)$ values based on measurement. The lowest average of $K_d(\lambda)$ values occurred on Panggang Island lagoon and the highest occurred on Air Island (Table 3-1).

The increased value of $K_d(\lambda)$ occurred in areas which was close to the coastal and in the middle of the lagoon area. This was probably due to the high concentration of chlorophyll-*a* and caused the increased absorption (Prasetyo *et al.* 2017). It might be caused by run off the organic and inorganic matters from Island and high waves caused the stirring of bottom substrate that dominantly consists of sand and other inorganic matters. Meanwhile, in the middle area of lagoons $K_d(\lambda)$ were increased.

Table 3-1: The averages of $K_d(\lambda)$ values on three areas of measurement (m^{-1}) (*)

	Air island		**Panggang island**		**Karang Lebar**	
	K_d (PAR)	K_d (380 – 890)	K_d (PAR)	K_d (380 – 890)	K_d (PAR)	K_d (380 – 890)
Lowest	0.235	0.319	**0.036**	**0.204**	0.166	0.252
Highest	**0.441**	**0.567**	0.322	0.622	0.431	0.592

(*) Summarized dataset from Prasetyo *et al.* (2017)

In the other hand, $K_d(\lambda)$ was decreased in the outside lagoon to open water (Nababan *et al.* 2013). These circumstances were described by Brown *et al.* (2008), where the open waters have optical properties, which influenced by organic matters like Chl-a rather than inorganic matters like TSS.

Based on in-situ measurement of Chl-a, Prasetyo *et al.* (2017) stated out that a high average of Chl-a values occurred on Panggang Island lagoon and the lowest was on Air Island. Based on TSS measurement, the high average of TSS values occurred on Karang Lebar lagoon and the lowest was on Panggang Island lagoon. Measurement of Kd(λ) values showed that light penetration on each sites was different. The lowest Kd(λ) values showed clearest water. Kd(λ) was a part of AOP, so the composition of organic and inorganic matters in water column has a great influence to penetrate the light on water column (Kirk 2011).

Shallow waters have a specific characteristic. When Chl-a concentration and TSS were high, it affects the absorption and scattering of light penetration through the water column (Saulquin *et al.* 2013). Wang *et al.* (2008) stated that $K_d(\lambda)$ was influenced by absorption coefficient from water molecules and distribution of light field on its water constituent.

According to Prasetyo *et al.* (2017) the Chl-a measurement in this study site has positive linear relationship with ratio of $K_d(\lambda)$ on λ = 443 nm and λ = 555 nm. The linear equation $K_d(443)/ K_d(555)$ = 2,774(Chl-*a*) + 0,4537 and it has high determination coefficient (R^2) of 0,8089 (Figure 3-1a). Meanwhile TSS has no positive relationship with $K_d(\lambda)$, where $K_d(550)$ has no significant relationship to TSS showed by *p-value* = 0,378 > 0,005 (Figure 3-1 b). $K_d(\lambda)$ values on 550 nm wavelength was used to calculate scattering coefficient of TSS (Petzold 1972; Budhiman *et al.* 2012). Scattering itself was dominantly influenced at longer wavelength (>510 nm) and absorption coefficient dominantly influenced at shorter wavelengths (Tiwari and Shanmugam 2013).

$K_d(\lambda)$ values is one of AOP part, and has a relationship with remote sensing reflectances, $R_{rs}(\lambda)$, where $K_d(490)$ has an empirical relationship with $R_{rs}(\lambda)$ ratio ($R_{rs}(490)/R_{rs}(555)$). The higher water constituent as part of AOP asymptotically influences the empirical approach. It was used to assess the characteristic of optical properties, which influenced by absorption of Chl-a and water molecules. An analysis of $K_d(490)$ with ratio $R_{rs}(490)/R_{rs}(555)$ then can be done using an empirical model developed by Lee *et al.* (2005) where the empirical model is appropriate to be applied to the dominant area influenced by absorption rather than scattering.

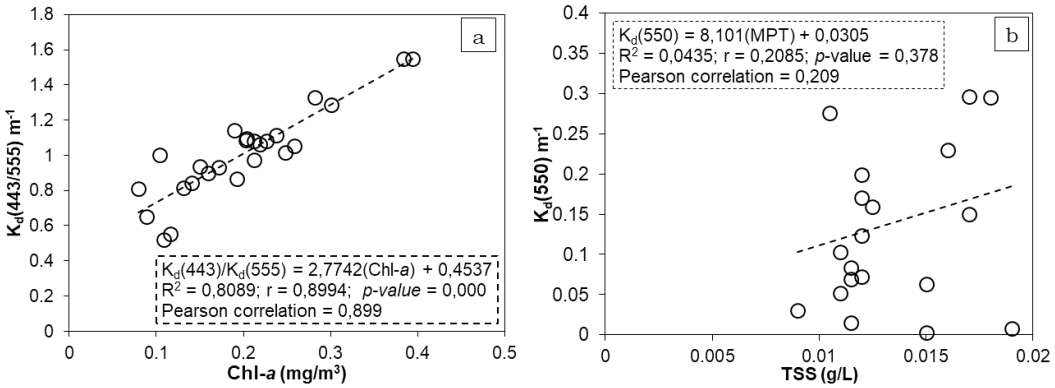

Figure 3-1: Graph of linear relationship between Chl-a and TSS against $K_d(\lambda)$ values at a specific wavelengths. (a) Chl-a and (b) TSS (Prasetyo *et al.* 2017)

The empirical models above was used to describe the relationship between the $R_{rs}(\lambda)$ at blue and green wavelength region with a simple regression to assess the correlation between the values of $K_d(490)$ with water-leaving radiance at blue wavelength region (λ = 443 nm) and green (λ = 555 nm). That empirical model was used to derive $K_d(490)$ from Sea-Viewing Wide Field-of-view (SeaWiFS) sensors (Austin and Petzold 1981; 1986, Morel 1986, Smith and Baker 1981, Mueller and Trees 1997). $K_d(490)$ was assumed to have correlation with pure water attenuation coefficient ($K_w(490)$ = 0,016 m^{-1}). The equation can be written as follows:

$$K_d(490) = K_w(490) + A\left(\frac{L_w(\lambda_1)}{L_w(\lambda_2)}\right)^B \qquad (3\text{-}1)$$

with A and B is constant, and $K_w(490)$ is attenuation coefficient for pure sea water. Then Mueller (2000) stated that water-leaving radiances (L_w) at blue and green wavelength region were suitable with the dataset provided by SeaWiFS at 450 nm and 555 nm sequentially. The equation 3-1 than can be rewritten as follows:

$$K_d(490) = K_w(490) + 0{,}15645\left(\frac{L_w(490)}{L_w(555)}\right)^{-1{,}5401} \qquad (3\text{-}2)$$

Lee *et al.* (2005) also stated that remote sensing reflectance (R_{rs}) can be calculated from the ratio of water-leaving radiance with downwelling irradiance that measured just above the surface, with the E_d ratio was at $E_d(490)$ and $E_d(555)$. Note that $E_d(490)/E_d(555)$ acquired from field measurement was only slightly around 1,3 occurred on this research on various sun angles, so the E_d ratio is set to constant, then the equation 3-2 can be rewritten as follows:

$$K_d(490)_{derived} = K_w(490) + 0{,}15645\left(1{,}3\frac{R_{rs}(490)}{R_{rs}(555)}\right)^{-1{,}5401} \qquad (3\text{-}3)$$

The equation above (equation 3-3) on can be used to calculate $K_d(490)$ values that derived from R_{rs} that measured from above water. The results then can be used to see the difference between derived $K_d(490)$ and measured $K_d(490)$. Linear regression graph on Figure 3-2 described the correlation.

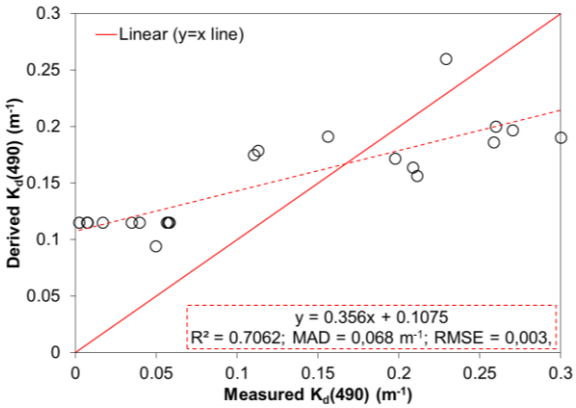

Figure 3-2: Derived $K_d(490)$ from empirical models developed by Lee *et al.* (2005) with the $K_d(490)$ values from the in-situ measurement

Based on Figure 3-2, it can be interpreted that in-situ measurement of $K_d(490)$ that had been done by Prasetyo *et al.* (2017), has a correlation with $K_d(490)$ that derived from Lee's empirical model from ratio $R_{rs}(490)$ and $R_{rs}(555)$. The determination coefficient (R^2) is 0,706 and RMSE = 0,003. Based on Figure 3-2, it is also shown that in three different area of in-situ measurement, there were overestimation on $K_d(490)$, so the plot moves away from 1:1 line approach to the derived $K_d(490)$ section on the graph. This analysis result was the opposite of what Lee *et al.* (2005) found, where the empirical methods to derive $K_d(490)$ has underestimate results towards the $K_d(490)$ from the in-situ measurement. It was happened because the results of ratio $R_{rs}(490)/R_{rs}(555)$ from empirical models describe earlier was used to calculate the attenuation change caused by absorption from water molecules and chlorophyll-a

concentration. While the results on Lee *et al.* (2005) studies occured because the in-situ measurement of $K_d(490)$ was conducted in an area that dominantly influenced by scattering coefficient.

From these analysis, it can be concluded that this study area was affected dominantly by absorption rather than scattering. It refers to the simple regression analysis between $K_d(443)$ and $K_d(555)$ and the $K_d(490)$ model developed by Lee *et al.* (2005).

3.2 Depth Estimation Based on $K_d(\lambda)$

Depth estimation using the algorithm developed by two ratio band from satellite image was a constant value of diffuse attenuation coefficient $K_d(\lambda)$ (Green *et al.* 2000). The datasets of $K_d(\lambda)$ from Prasetyo *et al.* (2017) then used to developed depth estimation algorithm using $K_d(\lambda)$ that simulated with center wavelength on Landsat 8. The simulated center wavelength then used for $K_d(\lambda)$, it was described in Table 3-2.

Table 3-2: Simulated center wavelength of Landsat 8 that used to estimates depth using $K_d(\lambda)$ values

No Band	Band	Landsat 8 (nm)	$K_d(\lambda)$ (nm)
1	*Coastal Blue*	435 - 451	442,96
2	*Blue*	452 - 512	482,04
3	*Green*	533 - 590	561,41
4	*Red*	636 - 673	654,59

$K_d(\lambda)$ ratio value from the simulated center wavelength was done by three simple linear functions, i.e. linear, logarithmic and exponential (Figure 3-3). The graph of the $K_d(\lambda)$ ratio showed that ratio between $K_d(442,96)$ and $K_d(482,04)$ has no significant relationship with depth from in-situ measurement with the plot moved away from the trendline. Meanwhile, the other ratio has significant relationship on each function with the plot moved near to the trendline (Figure 3-3). The models and determinations coefficient of each function described in Table 3-3.

Based on estimation algorithm using $K_d(\lambda)$ values (Figure 3-3 and Table 3-3) the best model fit was with exponential function with R^2 = 0,808 on the ratio $K_d(\lambda)$ at wavelength 442,96 nm and 654,59 nm, and the logarithmic function on the ratio at wavelength 482,04 nm and 654,59 nm. It is in accordance with the Beer-Lambert law that diffuse attenuation coefficient has an exponential relationship with the depth.

The reason for the exponential model was chosen because it was more consistent in generating depth estimation than the logarithm model, although the coefficient of determination value of the logarithmic model is larger than exponential. The model was selected also because of the accuracy test from both models, the exponential model has value of RMSE = 0.224 and MAPE = 3.72%, compared to the logarithmic models (RMSE = 0.582 and MAPE = 11.83%).

For additional note, if the value of the ratio $K_d(\lambda)$ increased then the depth sensed by the optically based sensor will get smaller, which is caused by the interruption of electromagnetic waves, when penetrating the water column. Due to the attenuation processes, the electromagnetic waves detected by the sensors, were already experiencing the interaction with water constituent and the water molecules itself (Groetsch 2011). The ratio of $Kd(\lambda)$ values occurs in the blue and red wavelength region, where the attenuation in the red region will be greater than in the blue region, it corresponds to Bukata *et al.* (1995).

We found in the several locations of $K_d(\lambda)$ measurement based on Prasetyo *et al.* (2017) dataset, the values that cannot be used to construct a model of depth estimation becomes outliers. There are seven locations that became outliers,

which were station 1, 21, 22, 24, 27, 29 and 30. If these locations were used as inputs to construct the model, the determination coefficient from models become small and the plots became be increasingly moving away from trendline. There was inconsistency on the models if $K_d(\lambda)$ values influenced by the reflection or reflectance from bottom objects (sand, mud, coral bleach, etc) significantly. It occurred because the measurement was conducted in the shallow waters. An inconsistent of $K_d(\lambda)$ model values on estimating depth caused the accuracy of the models to decrease.

Based on the model, it also showed the smaller the ratio of $K_d(\lambda)$ values, the more depth value can be calculated and estimated based on the measurement of downwelling irradiance, $E_d(\lambda)$. Exponential model of $K_d(\lambda)$ values towards depth from in-situ measurement showed that it has an empirical relationship, (Figure 3-3 and Table 3-3). $K_d(\lambda)$ values can be used as inputs to developed a model to calculate depth of the water column based on light penetration (Groetsch and Gege 2012).

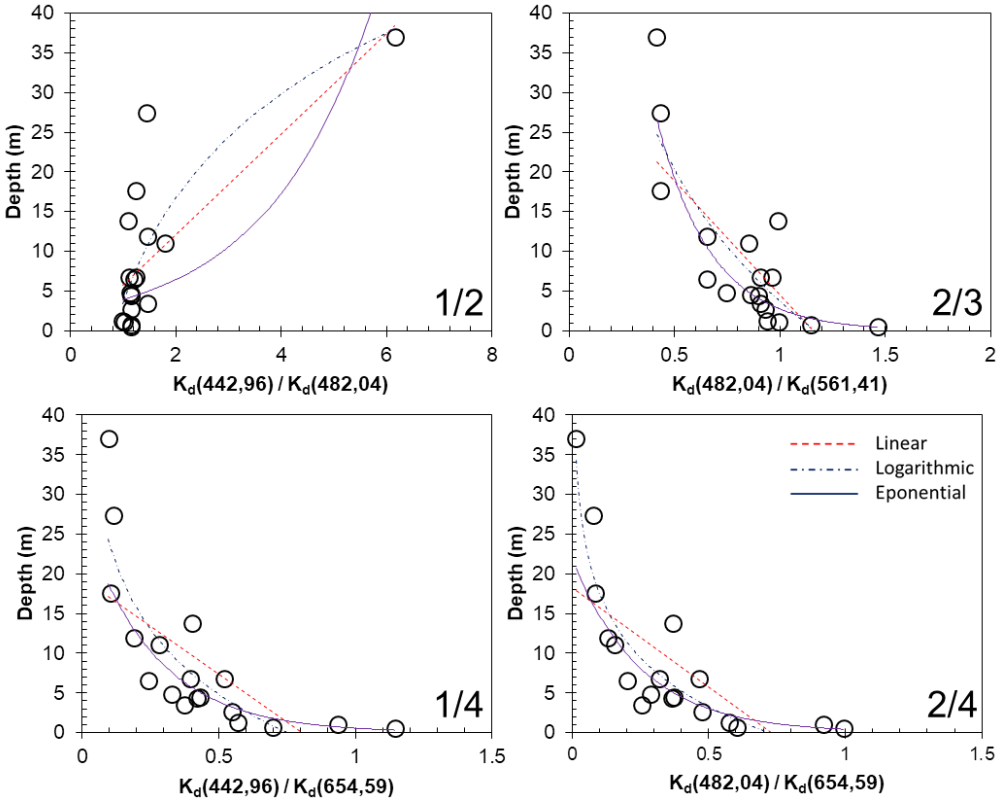

Figure 3-3: Ratio of two specific wavelengths of $K_d(\lambda)$ values towards water column depth

Tabel 3-3: Depth estimation models from $K_d(\lambda)$ values ratio

$K_d(\lambda)$ Ratio Simulated Band	Model					
	Linear	R^2	Logarithmic	R^2	Exponential	R^2
442.96/482.04 **1/2**	Z = 6.3127*[1/2] - 0.499	0.571	Z = 18.963*ln[1/2] + 3.5287	0.621	Z = 2.39 0.495*[1/2]	0.231
482.04/561.41 **2/3**	Z = -28.65*[2/3] + 33.2	0.583	Z = -23.97*ln[2/3] + 3.7295	0.699	Z = 135.19 -3.898[2/3]	0.708
442.96/654,59 **1/4**	Z = -24.186*[1/4] + 19.512	0.473	Z = -11.89*ln[1/4] - 3.4158	0.731	**Z = 27.346 -3.9[1/4]**	**0.808**
482.04/654,59 **2/4**	Z = -25.022*[2/4] + 18.299	0.479	Z = -8.97*ln[2/4] - 2.9623	0.845	Z = 22.067 -3.983[2/4]	0.798

The previous study about the relationship between water depth and diffuse downwelling attenuation coefficients was used to determine the current sensor depth from under water downwelling irradiance measurements using that model combined with improved parameterizations for the diffuse downwelling attenuation coefficients. The previous study stated out that the method for determination of depth from downwelling irradiance can produce results to investigated depth based on light penetration (Groetsch and Gege 2012). The difference between this research and the previous research was the parameterization of the model using analytical approach which had a better and accurate results of depth estimation compared to this research that only used an empirical approach.

3.3 Depth Estimation Based on Band Ratio of Landsat 8

Depth estimation algorithm using Landsat 8 imagery was conducted by using in-situ depth measurement as input towards band ratio from Landsat 8 reflectance. Landsat 8 band ratio's test performed on band 1 to 4 where the combinations of each band has a better sensitivity towards the increased depth. The reason these bands were used was that the reflectance on coastal blue band and blue band (435 – 512 nm) decreased rapidly towards the depth. This method was in accordances with previous research (Jagalingam *et al.* 2015; Stumpf *et al.* 2003).

After the satellite images were corrected (geometric, radiometric and atmospheric), the ratio of reflectance values then used to generate the algorithm mentioned earlier (equation 2-4). The test of band ratio was performed with certain criteria applied. The shorter wavelength as the numerator, and longer wavelength as the denominator. The test results of each band ratio towards depth from in-situ measurement generate an algorithm for each ratio as shown in Figure 3-4.

The test result for each band ratio showed that ratio of Band 1 and Band 3 provide good relationship (R^2 = 0,6115) compared to others band ratio. It happened due to the insufficient dataset. The algorithm built by band ratio 1 and 3 is more appropriate for estimating the water column depth using Landsat 8 imagery (Figure 3-4).

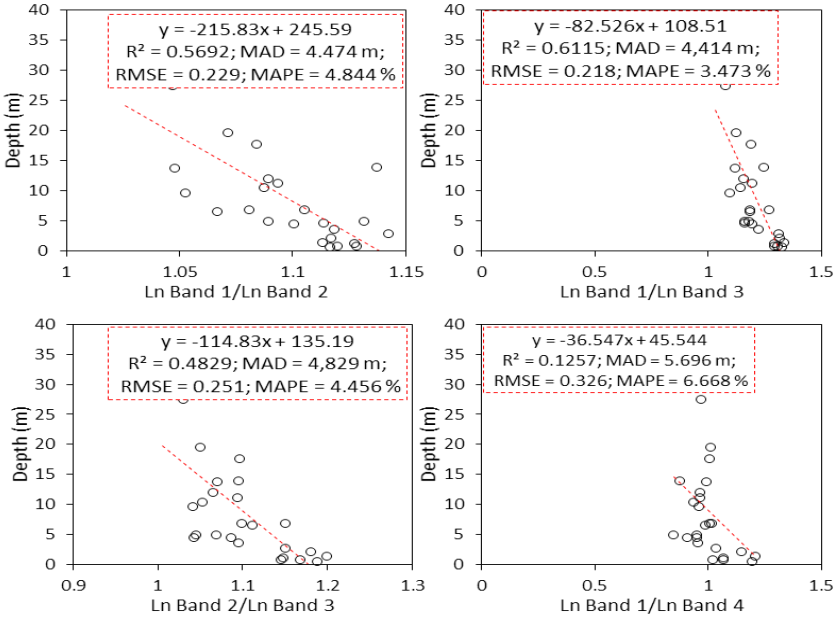

Figure 3-4: Graph of band ratio towards depth from in-situ measurement

Between another band ratio, band ratio 1 and 3 and band ratio 1 and 2 performed better to estimate depth (Fig. 3-4). Accuracy test was performed for all band ratios against estimated depth by calculating the value of Mean Absolute Deviation (MAD), Root Mean Square Error (RMSE) and Mean Absolute Percentage Error (MAPE). The accuracy test is shown in Figure 3-4.

The error on depth estimation of each band caused by the difference of spectral response against different bottom types. It is known in the area around the Karang Lebar lagoonal area that there are many different types of substrates. The substrate itself dominated by sand, which has greater reflectance value, compared to the others bottom types such as coral reef and macroalgae (Subarno *et al.* 2015). The previous research to estimate depth using satellite imagery by Loomis, (2009) also stated out that splitting the bottom types could increase the accuracy.

3.4 A Comparison of the Results of Estimated Depth Using Landsat 8 Imagery and $K_d(\lambda)$ Values

Based on the depth estimation algorithm using Landsat 8 image and $K_d(\lambda)$ value, the estimation result of the two methods was then compared to see the accuracy and proximity to the in-situ measurement results. By calculating MAD, RMSE and MAPE, the best algorithm was chosen from two methods to estimate the depth. The algorithm on Landsat-8 band ratio was for band 1 and 3 (blue and green region), meanwhile, the algorithm selected from $K_d(\lambda)$ values was the ratio between 442,96 nm and 654,59 nm (blue and red region). Both algorithms were selected based on the accuracy test with in-situ measurement. The selected algorithm based on $K_d(\lambda)$ ratio were caused by the attenuation of the water column at the red region having the greatest absorption compared with the blue region. These two wavelengths were attribute to the attenuation caused by absorption of water constituent and the depth range of water column (Morel 1988).

Band ratio algorithms from both methods had better determination coefficient compared to the rest. The result of depth estimation using both methods is shown in Table 3-4.

Tabel 3-4: Depth estimation based on band ratio of Landsat 8 and $K_d(\lambda)$ values (*meters*)

Station	In-situ Measurement	Landsat (*)	Ratio $K_d(\lambda)$ (**)
6	27.40	19.469	17.491
9	4.50	12.609	5.100
10	4.80	10.800	7.637
12	17.60	10.329	18.177
13	6.50	10.602	10.562
14	2.70	0.034	3.212
15	1.10	1.608	0.714
16	6.80	10.383	3.575
17	13.80	5.598	5.640
18	11.90	12.697	12.995
19	6.80	3.535	5.819
20	4.40	9.757	5.274
23	11.10	9.775	9.139
25	3.50	7.398	6.355
26	0.70	1.752	1.798
28	1.30	-1.703	2.949
31	37.00	23.413	18.770
32	0.50	-1.011	0.314

*) Band ratio 1 and 3 from Landsat 8 imagery
**) Ratio of center wavelength $K_d(\lambda)$ values, $K_d(442.96)$ and $K_d(654,59)$

In order to know the best result of estimation using two algorithm, several test were then performed. The result showed that the algorithm of depth estimation based on $K_d(\lambda)$ values was better than estimation based on Landsat 8 band ratio (Table 3-5).

Table 3-5: Accuracy test for both method to estimate the depth of water column

Accuracy test	Landsat 8	$K_d(\lambda)$
MAD	4.565 m	3.289 m
RMSE	0.314	0.307
MAPE	3.812 %	1.884 %

The results of depth estimation based on $K_d(\lambda)$ band ratio and in-situ measurement then interpolated into contour map. It was then compared visually. Based on a contour map of estimated depth using ratio from $K_d(\lambda)$ values on two wavelengths, it had a similar pattern between the depth from in-situ measurement (Figure 3-5). Visually, the contour map between in-situ measurement and estimated depth by $K_d(\lambda)$ values had similar pattern. An analysis was then conducted on the variances between these data. The result showed that the two data were not significantly different, showed by F = 0,563 < F critical = 4,042.

There were still some inconsistency when depth estimation using a ratio of $K_d(\lambda)$ applied directly to the shallow waters. The inconsistency would caused the results of estimation become over-estimate. It might be happened because of the optical characteristic on shallow waters still predominantly influenced by the reflection of bottom albedo, especially when the shallow waters had a high clarity and a high reflection of light. It made the attenuation depth increased even further from the actual water column depth.

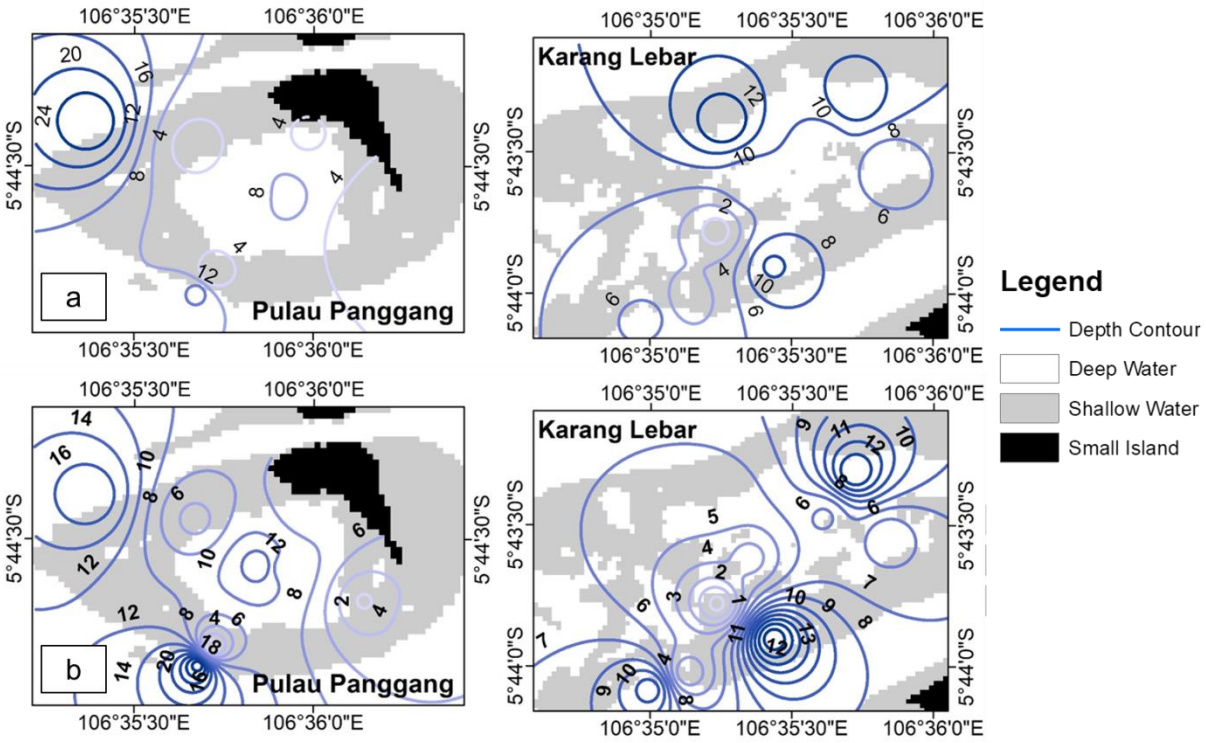

Figure 3-5: Contour map of estimated depth; (a) depth from in-situ measurement; (b) estimated depth by $K_d(442.96)$ and $K_d(654,59)$ ratio

4 CONCLUSION

This study showed the relationship between $K_d(\lambda)$ from in-situ measurement was the occurence of absorption dominantly by chlorophyll-*a* concentration at the blue and green spectral wavelength compared to the scattering by TSS. Depth estimation based on band ratio from in-situ measurement of $K_d(\lambda)$ occured at 442,96 nm and 654,59 nm, which had better estimation compared to Landsat 8 band ratio using band 1 and 3. Depth estimated based on $K_d(\lambda)$ band ratio and in-situ measurement were not significantly different. However, depth estimation based on $K_d(\lambda)$ band ratio was inconsistent due to bottom albedo reflection because the $K_d(\lambda)$ measurement was carried out in shallow waters. Depth estimation based on $K_d(\lambda)$ ratio had better results compared to the Landsat 8 band ratio showed by the accuracy test to both methods. Depth estimation using $K_d(\lambda)$ value on a certain wavelength was potential to be done based on the light penetration in the water column by empirical approach.

ACKNOWLEDGEMENTS

We thank the Director of Remote Sensing Applications Center of LAPAN, Dr. M. Rokhis Komaruddin that gave permission to take part on in-situ measurement activities in Seribu Island, DKI Jakarta. We also thank Mr. Syarif Budhiman who gave the author advice as well as permission to use the spectroradiometer TriOS-RAMSES.

REFERENCES

[APHA] American Public Health Association, (2012), Standard Methods for the Examination of Water and Waste Water. 22nd edition. Washington (US): APHA.

[USGS] United States Geological Survey, (2015), Landsat 8 data users handbook. Department of interior. U.S. Geological Survey. LSDS-1574 Version 1.0.

Austin RW, Petzold TJ, (1981), The Determination of the Diffuse Attenuation Coefficient of Sea Water Using the Coastal Zone Color Scanner. *J.F.R. Garver. Oceanography from Space*. Springer. 239-256.

Austin RW, Petzold TJ, (1986), Spectral Dependence of the Diffuse Attenuation Coefficient of Light in Ocean Waters. J. Opt. Eng. 25: 473– 479.

Brown CA, Huot Y., Werdell PJ, Gentili B., Claustre H., (2008), The Origin and Global Distribution of Second Order Variability in Satellite Ocean Color and its Potential Applications to Algorithm Development. *J. Remote Sens. Environ.* Vol 112:4186-4203.

Budhiman S., Salama MS, Vekerdy Z., Verhoef W., (2012), Deriving Optical Properties of Mahakam Delta Coastal Waters, Indonesia using in situ measurements and ocean color model inversion. *ISPRS Journal of Photogrammetry and Remote Sensing* 68: 157-169.

Bukata RP, Jerome JH, Kondratyev Kya, Pozdnyakov DV, (1995), Optical Properties and Remote Sensing of Inland and Coastal Waters. CRC press.

Green EP, Mumby PJ, Edwards AJ, Clark CD, (2000), Remote Sensing Handbook for Tropical Coastal Management. UNESCO Publishing, *p 121-128*

Groetsch P., (2011), Optimization and Verification of a New Analytical Radiative Transfer Model. [tesis]. Munchen (Germany): Deutschen Luft- und Raumfahrtzentrum.

Groetsch P., and Gege P., (2012), Determination of Sensor from Downwelling Irradiance Measurements. In Geoscience and Remote Sensing Symposium (IGARSS), IEEE International: 2860-2863

Jaelani MJ., Setiawan F., Wibowo H., Apip, (2015), Pemetaan Distribusi Spasial Kosentrasi Klorofil-a dengan Landsat 8 di Danau Matano dan Danau Towuti, Sulawesi Selatan. *Prosiding pertemuan tahunan masyarakat ahli penginderaan jauh Indonesia* XX. Bogor.

Jagalingam P., Akshaya BJ, and Hegde, AV, (2015), Bathymetry Mapping Using Landsat 8 Satellite Imagery. Procedia Engineering, 116, 560-566.

Kirk JTO, (2011), Light and Photosynthesis in Aquatic Ecosystem. Third Edition. Cambridge University Press, United Kingdom.

Lee ZP, Du KP, and Arnone R., (2005), A Model for the Diffuse Attenuation Coefficient of Downwelling Irradiance. Journal of Geophysical Research: Oceans, 110(C2).

Loomis MJ, (2009), Depth Derivation from the Worldview-2 Satellite Using Hyperspectral Imagery. Naval Postgraduate School, Monterey, California.

Lyzenga DR, (1978), Passive Remote Sensing Techniques for Mapping Water Depth and Bottom Features. Appl. Opt. J. 17(3):379-383.

Lyzenga DR, (1981), Remote Sensing of Bottom Reflectance and Water Attenuation Parameters in Shallow Water Using Aircraft and Landsat Data. Int.J.Remote Sensing 2(1): 71-82.

Mobley CD, (1994), Light and Water: Radiative Transfer in Natural Waters. San Diego: Academic Press.

Morel A., (1988), Optical Modeling of the Upper Ocean in Relation to its Biogenous Matter Content (Case I Waters). Journal of Geophysical Research 93(10):749-10.

Mueller JL, (2000), SeaWiFS Algorithm for the Diffuse Attenuation Coefficient, K(490), using water-leaving radiances at 490 and 555 nm, in Sea- WiFS Postlaunch Calibration and Validation Analyses, part 3, edited by S. B. Hooker, 24–27, NASA Goddard Space Flight Cent., Greenbelt, Md.

Mueller JL, Fargion GS, and McClain CR, (2003), Ocean Optics Protocols for Satellite Ocean Color Sensor Validation. Revision 4, Vol. I-VII, NASA, Goddard Space Flight Space Center, Greenbelt, Maryland.

Mueller JL, Trees CC, (1997), Revised SeaWiFS Prelaunch Algorithm for Diffuse Attenuation Coefficient K(490), NASA Tech. Memo., TM-104566, 41: 18– 21.

Nababan B., Louhenapessy VSA, Arhatin RE, (2013), Downwelling Diffuse Attenuation Coefficients from In-situ Measurement of Different Water Types, International Journal of Remote Sensing and Earth Science, 10(2): 122-133.

Petzold TJ, (1972), Volume Scattering Functions for Selected Natural Waters. *SIO Ref*, 72-78.

Prasetyo BA, Siregar VP, Agus SB, Asriningrum W., (2017), Pengukuran Koefisien *Diffuse* Atenuasi (K_d) di Perairan Dangkal Sekitar Karang Lebar, Kepulauan Seribu, DKI Jakarta, Jurnal Teknologi Perikanan dan Kelautan, (in press).

Saulquin B, Hamdi A, Gohin F, Populus J, Mangin A, d'Andon OF, (2013), Estimation of the diffuse attenuation coefficient K_dPAR using MERIS and application to seabed habitat mapping. *J. Remote Sensing of Environment* 128: 224-233.

Siregar VP, Selamat MB, (2010), Evaluasi Citra Quickbird untuk Pemetaan Batimetri Gobah dengan Menggunakan Data Perum: Studi Kasus Gobah Karang Lebar dan Pulau Panggang. J. Ilmu Kelaut. 2: 99-109.

Smith RC, and Baker KS, (1981), Optical Properties of the Clearest Natural Waters, Appl. Opt., 20: 177– 184.

Stumpf RP, Holderied K., (2003), Determination of Water Depth with High-Resolution Satellite Imagery Over Variable Bottom Types. Limnol. Oceanogr. 48(1, part 2): 547-556.

Subarno T., Siregar VP, Agus SB, (2015), Evaluasi Citra Worldview-2 untuk Pendugaan Kedalaman Perairan Dangkal Pulau Kelapa-Harapan Menggunakan Algoritma Rasio Band. Journal of Geomatics and Planning. 2(1): 30-37.

Tiwari SP, Shanmugam P., (2013), An Optical Model for Deriving the Spectral Particulate Backscattering Coefficients in Oceanic Waters. *Ocean Science*, *9*(6): 987-1001.

Vanderstraete T., Goosens R., and Ghabour TK, (2004), Coral Reef Habitat Mapping in the Red Sea (Hurghada, Egypt) Based on Remote Sensing. Paper presented at the EARSel eProceedings, Strasbourg, France, 191-207.

Wang G., Cao W., Yang D., and Xu D., (2008), Variation in Downwelling Diffuse Attenuation Coefficient in the Northern South China Sea. Chinese Journal of Oceanology and Limnology, 26(3): 323-333.

Zheng Z, Ren J., Li Y., Huang C., Liu G., Du C., and Lyu H., (2016), Remote Sensing of Diffuse Attenuation Coefficient Patterns from Landsat 8 OLI Imagery of Turbid Inland Waters: A case study of Dongting Lake. Science of the Total Environment, 573, 39-54.